

Preparation and Performance of High Activation Carbon Microbeads for Application of Supercapacitors

Li Bai, Xingyan Wang, Xianyou Wang*, Xiaoyan Zhang, Wanmei Long, Hong Wang and Xiaoshuan Li

Key Laboratory of Environmentally Friendly Chemistry and Applications of Minister of Education, School of Chemistry, Xiangtan University, Hunan, Xiangtan 411105, China

Received: March 26, 2011, Accepted: April 29, 2011, Available online: October 13, 2011

Abstract: Carbon microbeads (CMB) were successfully prepared by glucose hydrothermal route in a stainless steel autoclave. The CMB was treated in concentrated nitric acid in order to gain the highly activated carbon microbeads (ACMB). The structure and surface morphology of as-prepared ACMB were characterized by scanning electron microscopy (SEM) and Fourier transform infrared spectrometer (FTIR), respectively. The electrochemical characteristics and capacitive behaviors of the ACMB were studied by cyclic voltammetry, galvanostatic current charge/discharge and cycle life measurements. The results show that the ACMB electrode has good electrochemical performance and the specific capacitance of ACMB is 291.9 F g^{-1} at a scanning rate of 1 mV s^{-1} . Meanwhile, the specific capacitance of the button supercapacitor was as high as 75 F g^{-1} at a charge/discharge current density of 0.5 A g^{-1} and the loss of specific capacitance was nearly neglectable after 5000 cycles.

Keywords: Carbon microbeads; Hydrothermal route; Supercapacitor; Electrochemical performance

1. INTRODUCTIONS

Supercapacitor is a type of energy storage device with features intermediate between conventional dielectric capacitors and batteries. They have many attractive characteristics such as low equivalent series resistance (ESR), rapid charge/discharge, long cycle life and high power density. Due to these properties, potential applications of supercapacitor include loading leveling functions for batteries in electric vehicles during starting, acceleration and regenerative braking and burst power generation in electronic devices such as cellular phones, camcorders and navigational devices [1-3].

In supercapacitor, energy is stored in terms of both double-layer and pseudo-capacitance. Carbon materials with relatively low cost, high surface area, high specific capacitance and long cycle life are widely used for double layer capacitors, which utilize the capacitance arising from charge separation at an electrode/electrolyte interface. Various carbon materials such as activated carbon, carbon fibers, carbon aerogels, mesoporous carbon, carbide-derived carbon (CDC) and carbon microbeads have been identified as

possible electrode materials for a high power and higher energy density supercapacitor [4-9]. Of these, carbon microbeads are a kind of potential electrode material for supercapacitor, and they have several advantages such as high electrically conductivity, good fluidity, excellent sphericity, easy to control pore size distribution and a relatively low cost [10-11].

To date, carbon microbeads have been prepared via various methods, such as chemical vapor deposition, template, arc discharge, hydrothermal [12-15] and so forth. Among all kinds of methods that can be employed for preparation of carbon microbeads, hydrothermal method is a promising and innovative technology because of its safe non-toxic, simple technologies and higher purity product. Recently, there have some reports that biological materials are used to prepare the carbon microbeads by hydrothermal method, such as glucose, sucrose and fiber [15-16]. Mi [15] et al. reported that carbon micro-spheres can be prepared with the aqueous glucose solution as starting materials in a stainless steel autoclave at $500 \text{ }^\circ\text{C}$ for 12 h. The carbon micro-spheres have regular and perfect shape, high yields and narrow-range distributions, and diameters ranging from 1 to $2 \text{ }\mu\text{m}$. Wang [16] et al. prepared hard carbon with sugar as the precursor by

*To whom correspondence should be addressed: Email: wxianyou@yahoo.com
Phone: 86-731-58292060, Fax: 86-731-58292061

hydrothermal method. The resultant hard carbon has perfect spherical morphology and uniform nanopores of about 0.4 nm in diameter. However, very few studies were reported to use the carbon microbeads as electrode material of supercapacitor until now.

In this paper, the CMB was prepared by glucose hydrothermal method and carbonized in a tube furnace in argon atmosphere. The CMB was treated in concentrated nitric acid in order to gain ACMB. The as-prepared ACMB were characterized by SEM and IR. Furthermore, the electrochemical behaviors of ACMB as the electrode of supercapacitor were investigated by cyclic voltammetry, galvanostatic current charge/discharge and cycle life measurements.

2. EXPERIMENTS

2.1. Materials

All the materials and chemical reagents were of analytical grade, such as glucose, ethanol, nitric acid solution which were obtained from commercial sources and directly used without any pretreatment. The water was distilled water.

2.2. Preparation of ACMB

In a typical experiment, 1.5 mol L⁻¹ aqueous glucose solution was filled in a stainless steel autoclave with a fill rate of 75 %. The autoclave was sealed and maintained at 160 °C for 18 h in an oven, then cooled to room temperature naturally. A brown precipitate was collected, washed with distilled water and absolute ethanol. The obtained sample was then dried in a vacuum oven at 80 °C for 12 h. The sample was carbonized at desired temperature 750 °C for 1h in a flow of Ar. In this way, the carbon microbeads (CMB) were obtained. Then the CMB was treated in concentrated nitric acid activation at 70 °C stirred for 24 h to form activated carbon microbeads (ACMB).

2.3. Evaluation of electrochemical properties

The mixture containing 80 wt.% ACMB, 10 wt.% acetylene black, and 10 wt.% polytetrafluoroethylene (PTFE) aqueous suspension (60%) was well mixed, and then pressed onto a nickel foam substrate (1.6×10⁶ Pa) that used as a current collector (area was 1.5 cm²), and then dried at 80 °C for 12 h. The electrochemical performances of the prepared electrodes were characterized by cyclic voltammetry (CV) and charge/discharge tests. The used electrolyte was 6 mol L⁻¹ KOH solution. The electrochemical experiments were carried out using a three-electrode cell, in which nickel foam substrate and the saturated calomel electrode via a Luggin capillary with a salt bridge were used as counter and reference electrodes. The cyclic voltammetry and the charge/discharge measurements at constant current were performed by means of electrochemical analyzer systems, CHI660 (CH Instruments, USA). The galvanostatic current charge/discharge and cycle life tests were carried out by potentiostat/galvanostat (BTS6.0, Neware, Guangdong, China) on button supercapacitor, and the symmetrical button supercapacitor were assembled according to the order of electrode-separator-electrode. All the measurements were carried out at room temperature.

2.4. Measurement techniques of structural characterization

(1) Scanning electron microscopy (SEM) (JSM-6610, JEOL) was

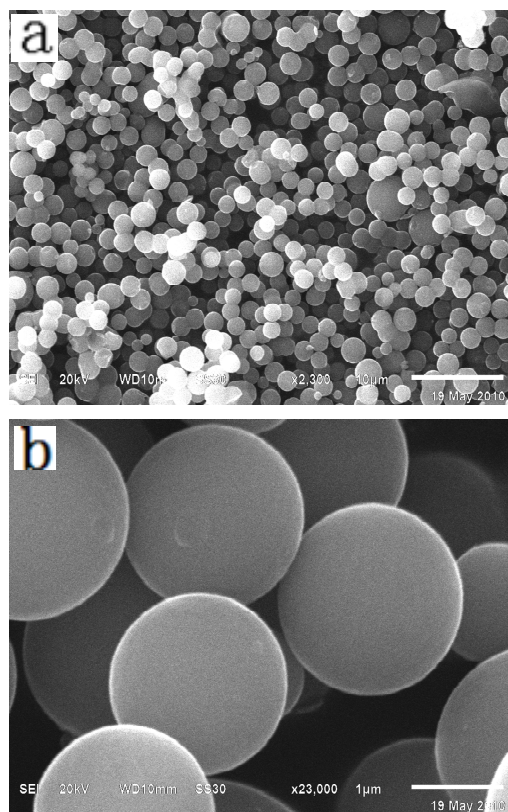


Figure 1. SEM images of ACMB

used to study the morphology and surface structure of the samples.

(2) The IR measurements of different samples were performed with a Fourier transform infrared (FTIR) spectrometer (Perkin-Elmer Spectrum one) in the wavelength range from 4000 to 500 cm⁻¹, using the KBr disk method.

(3) Sorption analysis of carbon material was done using N₂ as adsorbate at -196 °C with Quantachrome NovaWin2.

3. RESULTS AND DISCUSSION

3.1. Material characterization

Carbon microbeads are a kind of novel carbon materials with high electrical conductivity, good liquidity and other interesting properties. It has been reported that chemical or physical activation for carbon materials can improve their specific surface area, electrical conductivity and specific capacitance. Chen [17] et al. reported that the specific capacitance of carbon nanotube activated by concentrated nitric acid can increase from 40 to 68 F g⁻¹. Because the activation caused a slight enhancement in specific surface area and pore size. Besides, the oxygenous functions on the surface of material increased, which could improve the hydrophilicity and the capability to form electric double-layer. In this work, ACMB was obtained by treated CMB in concentrated nitric acid.

Fig. 1 shows SEM images of ACMB. It can be found that the final product is consisted of a large quantity of activated carbon microbeads with 1-2 µm in diameter, and the carbon microbeads have good dispersion and perfect spherical morphology.

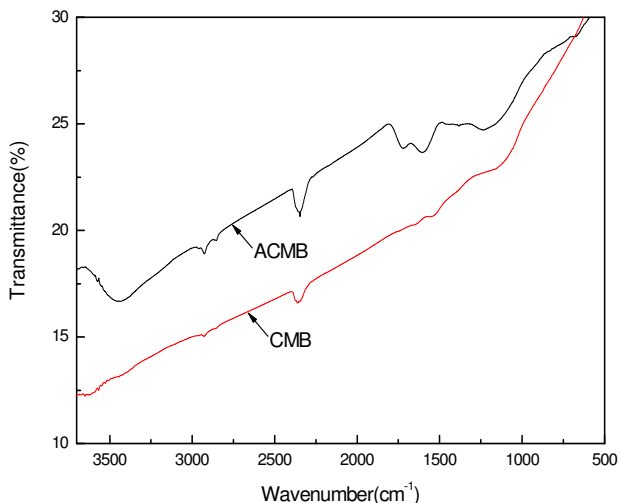


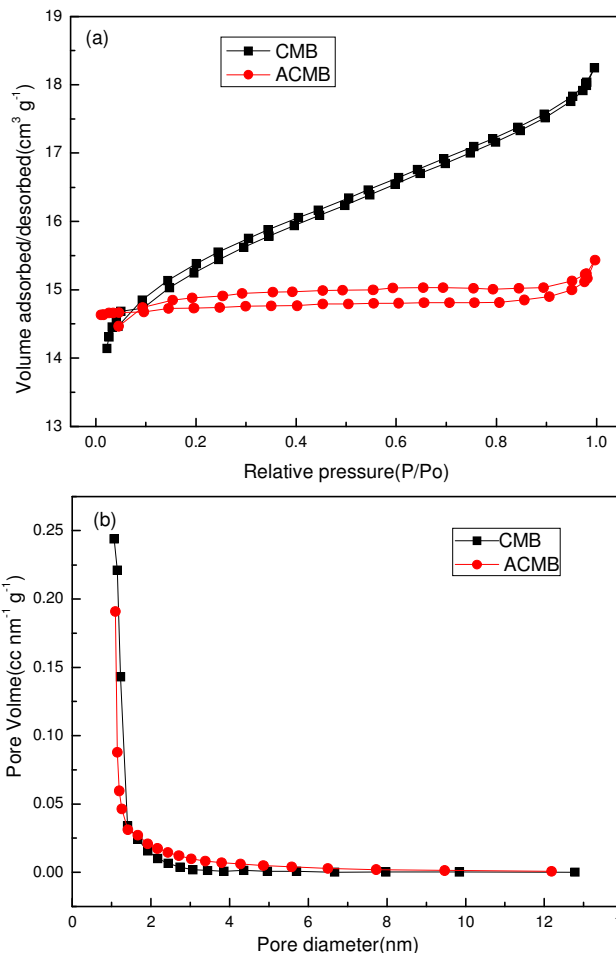
Figure 2. FTIR spectra of CMB and ACMB

The infrared spectra of CMB and ACMB are shown in Fig. 2. The broad band in 3451 cm^{-1} is assigned to $-\text{OH}$ stretching vibration. This bond may be attributed to the adsorbed water of the ACMB. The 2926 and 2847 cm^{-1} absorption bands belong to the CH_2 - stretching vibrations. The 1720 , 1604 cm^{-1} absorption bands, belong to the $\text{C}=\text{O}$ and aromatic rings stretching vibration, respectively. The absorption peak of methylene-ether ($\text{CH}_2\text{-O-CH}_2$) is observed at 1235 cm^{-1} . Compared IR spectra of the CMB and ACMB, it can be found that the functional groups of sample treated by HNO_3 were obvious changed, appearing in $-\text{OH}$ and $\text{C}=\text{O}$ stretching vibration peak, which mainly due to strong oxidation of HNO_3 . However, it is well known that an abundance of oxygen-containing functional groups of ACMB may provide a certain amount of pseudo-capacitance contributing to the improved capacitive performance.

Adsorption isotherm of N_2 gas was carried out in order to characterize the porous structure of the samples. Fig. 3 shows the typical N_2 adsorption/desorption isotherms at 77 K and the pore size distribution of both CMB and ACMB. The pore characteristics of CMB and ACMB are shown in Table 1. In Fig. 3a, a hysteresis loop was observed, which indicated that the structure of the ACMB was consisted of micropore and mesopore, and thus the ACMB was beneficial to electrolyte ion movement. The BET specific surface area, pore volume and pore size of CMB treated by HNO_3 increased remarkably because HNO_3 is strong acidic and strong oxidant, which can remove the impurities of the CMB; besides, nitric acid treatment can increase the nitrogen and oxygen-containing functional groups on the surface of carbon, which is beneficial to

Table 1. Characteristics of pore structure of CMB and ACMB

	BET-SSAa ($\text{m}^2\text{ g}^{-1}$)	Pore volume ($\text{cm}^3\text{ g}^{-1}$)	Average pore size (nm)
CMB	446.4	0.074	1.495
ACMB	494.6	0.093	1.536

Figure 3. Nitrogen adsorption isotherms at 77 K (a) and pore size distribution (b) of CMB and ACMB

increase redox pseudo-capacitance e of the CMB.

In order to further study on the change of element contents of CMB and ACMB, the elemental analysis was performed, and the results were tabulated in Table 2. As being seen from Table 2, the contents of carbon, nitrogen, oxygen increased after activated by concentrated nitric acid, therefore it was further confirmed that nitric acid treatment can increase in the numbers of nitrogen and oxygen functional groups on the surface of carbon.

3.2. Electrochemical characterization

The cyclic voltammogram was used in determination of electrochemical properties of the material. The specific capacitances of the electrode at different scanning rates in $6\text{ mol L}^{-1}\text{ KOH}$ was estimated from the following equation [3].

Table 2. The change of element contents of CMB and ACMB

	C	N	H	O	N/C
CMB	61.64	0.311	1.610	0.517	0.005
ACMB	66.79	1.400	1.614	1.357	0.021

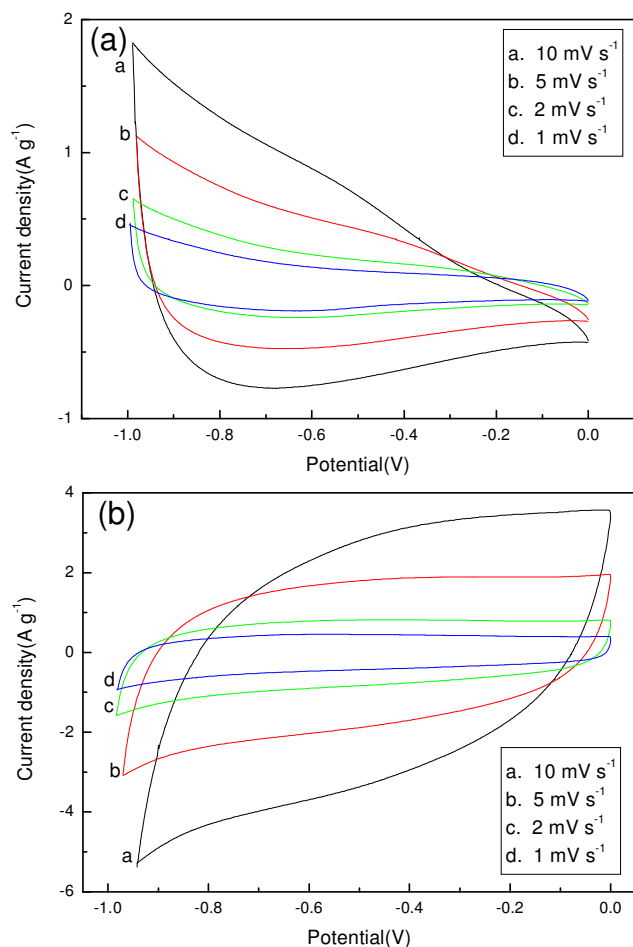


Figure 4. Cyclic voltammograms of CMB (a) and ACMB (b) at different scan rates

$$C = \frac{I_a + |I_c|}{2m(dV/dt)} \quad (1)$$

Where I_a , I_c , m and dV/dt are the currents of anodic and cathodic voltammograms on positive and negative scan, A, mass of the electrode material, g, and the scan rate, $V s^{-1}$, respectively.

Specific capacitances of ACMB and CMB electrodes with different scan rates are given in Fig. 4. The results are tabulated in Table 3. As being seen from Fig. 4 and Table 3 the CV curves of ACMB electrodes exhibit a rectangular-like shape, and the charging process is reversible in the scanning potential range, which is the typical characteristic for electric double layer capacitor. However, the CV

Table 3. Specific capacitance of CMB and ACMB within different scan rates

	10 $mV s^{-1}$	5 $mV s^{-1}$	2 $mV s^{-1}$	1 $mV s^{-1}$
CMB	67.8	85.4	102.5	134.6
ACMB	223.5	231.8	271.3	291.9

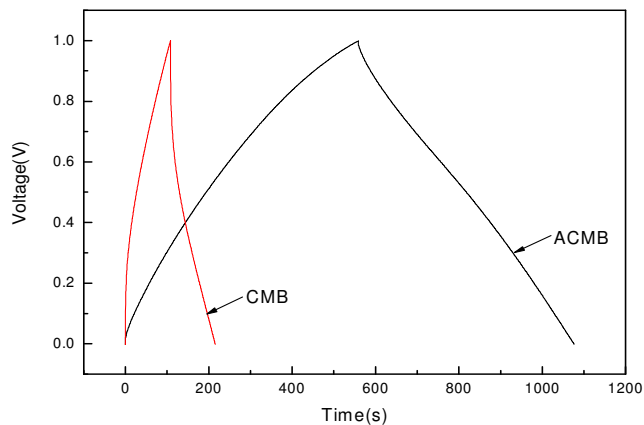


Figure 5. Charge/discharge curves of CMB and ACMB at current density of $0.5 A g^{-1}$

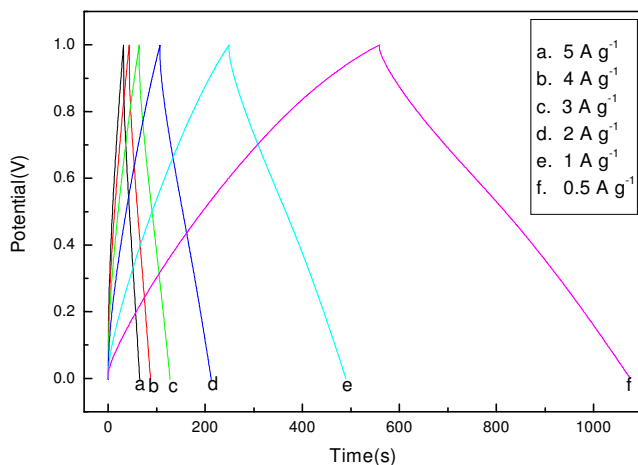


Figure 6. Charge/discharge curves of ACMB at different current densities

curves of CMB electrodes is distorted, and it is suggested that the reversibility of the CMB electrodes is not good in this potential range. The specific capacitance of ACMB electrode can reach $291.9 F g^{-1}$ at a scanning rate of $1 mV s^{-1}$. Besides, as the scan rate increases, the specific capacitance of ACMB electrode is gradually decreased. It may be that the electrolyte ions can easily transport in pores at the low scan rate; however, at high scan rate the electrolyte ions cannot availablely diffuse into the pores when each fast cycle is completed.

In order to gain a further understanding on the electrochemical performance of ACMB materials, the comparison of the charge/discharge curves for the CMB and ACMB electrode is shown in Fig. 5. It can be found that the charge/discharge curves of both CMB and ACMB have near isosceles triangle, which indicates that the charging/discharging processes of the electrode are reversible. In addition, it can also be seen that the charge/discharge curves of ACMB are almost linear, which indicates that ACMB has good capacitive properties.

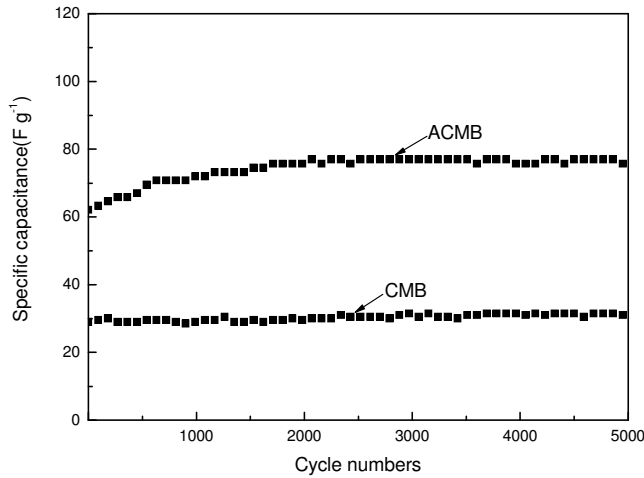


Figure 7. The cyclic life curve of CMB and ACMB supercapacitors at current density 0.5 A g^{-1}

The charge/discharge curves of the ACMB electrodes measured at different current densities within a potential window (0 to 1.0 V) are shown in Fig. 6. The specific capacitance of the supercapacitor can be evaluated from the charge/discharge test together with the following equation [18], and the results are tabulated in Table 4.

$$C = \frac{I \cdot \Delta t}{\Delta V \cdot m} \quad (2)$$

Where I , Δt , ΔV , m were the current used for charge/discharge, A, the time elapsed for the charge or discharge cycle, s, the voltage interval of the charge or discharge, V, the mass of activated carbon on the electrodes, g, respectively.

As being seen from Table 4 and Fig. 6, with the increase of current densities from 0.5 A g^{-1} to 5 A g^{-1} , the specific capacitance decreases from 261.0 F g^{-1} to 167.8 F g^{-1} . However, the specific capacitance for ACMB electrode is apparently higher than one of the CMB electrode at every given current density, which is in good agreement with the results of CV in Table 3.

The cyclic life curves of the CMB and ACMB supercapacitors are illustrated in Fig. 7. As shown in Fig. 7, the CMB and ACMB supercapacitors have demonstrated a very long cycle life under shallow depths of discharge, but the specific capacitance (30 F g^{-1}) of the CMB supercapacitor is clearly lower than the one (75 F g^{-1}) of the ACMB supercapacitor. Besides, the specific capacitance shows an initial increase of the ACMB supercapacitor at the beginning of the cycle, which mainly due to the active material of capacitors has a gradual activation process; specially for ACMB which was treated in HNO_3 , it appears a certain amount of surface

Table 4. Specific capacitance of CMB and ACMB within different current densities

	5 A g^{-1}	4 A g^{-1}	3 A g^{-1}	2 A g^{-1}	1 A g^{-1}	0.5 A g^{-1}
CMB	18.3	25.0	38.0	62.7	108.1	149.0
ACMB	167.8	172.0	193.2	211.8	241.7	261.0

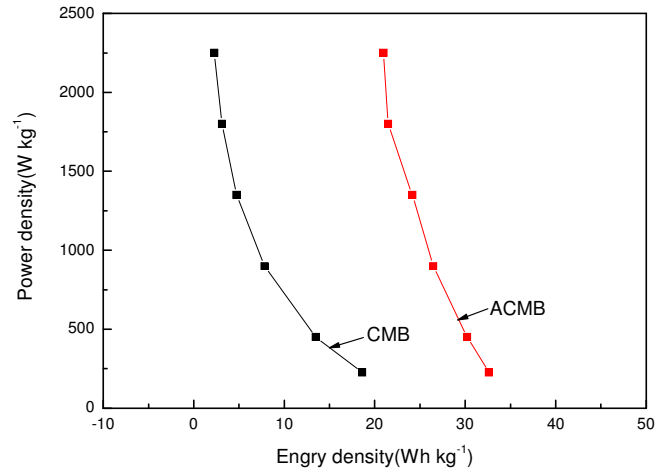


Figure 8. Ragone plot of the CMB and ACMB supercapacitors

functional groups, and these functional groups in the cyclic process need a certain period to form a stable structure. After 600 consecutive cycles, the capacitance of the ACMB supercapacitor fixed at a steady value (75 F g^{-1}). Even though it was continuously worked 5000 cycles, the loss of specific capacitance was nearly neglectable. ACMB is a kind of promising electrode active material for supercapacitors.

Fig. 8 is the Ragone plot of the CMB and the ACMB supercapacitors. Energy density and power density are calculated using Eqs.3 and 4 [19]:

$$E = \frac{1}{2} C (\Delta V)^2 \quad (3)$$

$$P = \frac{I \Delta V}{2m} \quad (4)$$

Where C is the capacitance of the capacitor, and it is calculated according to Eq.2; I , ΔV , and m represent discharge current, range of the charge/discharge, and mass of active materials, respectively.

The high capacitive performance of ACMB can also be observed in the Ragone plot presented in Fig. 8. The energy densities of the ACMB are obviously larger than that of the CMB. As the power density increases from 225 to 2250 W kg^{-1} , the energy density of ACMB drops from 32.6 to 21.0 Wh kg^{-1} . Besides, with the increase of the power density, the energy density of the ACMB supercapacitor decreases slightly slower than that of the CMB supercapacitor. Thus ACMB is promising for applications where high power outputs as well as high energy capacities are required, such as electric vehicles.

4. CONCLUSIONS

CMB were successfully prepared by glucose hydrothermal method and characterized for the application of supercapacitor. The ACMB have a regular and perfect spherical morphology, good dispersion, narrow-range distributions and diameters ranging from 1 to $2 \mu\text{m}$. Activation treatment in HNO_3 solution is an available

route to improve the capacitive performance of CMB. The specific capacitance of ACMB treated in concentrated nitric acid was as high as 291.9 F g^{-1} in 6 mol L^{-1} KOH electrolyte at a scanning rate of 1 mV s^{-1} , which was apparently higher than that of CMB electrode. The specific capacitance of the button supercapacitor with the ACMB as the electrode active materials was up to 75 F g^{-1} at a charge/discharge current density of 0.5 A g^{-1} . Besides, the ACMB supercapacitor has stable electrochemical properties, excellent reversibility and a long cycle life. Thus ACMB can be considered as a promising material for the application of supercapacitors.

5. ACKNOWLEDGEMENT

This work was financially supported by the National Natural Science Foundation of China (Grant No. 20871101), Doctoral Fund of Ministry of Education of China (Grant No. 20094301110005) and Key Project of Educational Commission of Hunan Province, China (Grant No.08A067).

REFERENCE

- [1] H.Q. Wang, Z.S. Li, J.H. Yang, Q.Y. Li, X.X. Zhong, *J. Power Sources* 194 (2009) 1218-1221.
- [2] B.E. Conway, *Electrochemical Super Capacitor and Technological Applications*, Kluwer Academic, Plenum Press, New York, 1999.
- [3] Q.H. Huang, X.Y. Wang, J. Li, *Electrochimica Acta* 52 (2006) 1758-1762.
- [4] C. Portet, P.L. Taberna, P. Simon, E. Flahaut, C. Laberty-Robert, *Electrochim. Acta* 50 (2005) 4174-4181.
- [5] W.C. Chen, C.C. Hu, C.C. Wang, C.K. Min, *J. Power Sources* 125 (2004) 292-298.
- [6] P.R. Kalakodimi, M. Norio, *Electrochem. Solid-State Lett.* 425 (2004) 7-11.
- [7] S.H. Yoon, S. M. Oh, C. Lee, *Mater. Res. Bull.* 42 (2009) 1663-1669.
- [8] L.P. Zheng, Y. Wang, X.Y. Wang, *J. Power Sources* 195(2010) 1747-1752.
- [9] J. Li, X.Y. Wang, Q.H. Huang, *J. Power Sources* 158 (2006) 784-788.
- [10] A.G. Pandolfo, A.F. Hollenkamp, *J. Power Sources* 157 (2006) 11-27.
- [11] Q.H. Huang, X.Y. Wang, J. Li, C.L. Dai, S. Gamboa, P.J. Sebastian, *J. Power Sources* 164 (2007) 425-429.
- [12] S.P. Yi, H.Y. Zhang, L. Pei, Y.J. Zhu, X.L. Chen, X.M. Xue, *J. Alloys Compd.* 420 (2006) 312.
- [13] Y. Liu, L. Zhan, R. Zhang, W.M. Qiao, X.Y. Liang, L.C. Ling, *New Carbon Mater.* 22 (2007) 259-261.
- [14] H.J. Huang, H. Kajiura, Y.S. Murakami, M. Ata, *Carbon* 41 (2003) 615-618.
- [15] Y.Z. Mi, W.B. Hu, Y.M. Dan, Y.L. Liu, *Mater. Lett.* 62 (2008) 1194-1196.
- [16] Q. Wang, H. Li, L.Q. Chen, X.J. Huang, *Carbon* 39 (2001) 12211-12214.
- [17] X.L. Chen, W.S. Li, C.L. Tan, W. Li, Y.Z. Wu, *J. Power Sources* 184 (2008) 668-674.
- [18] Y.G. Wang, H.Q. Li, Y.Y. Xia, *Adv. Mater.* 18 (2006) 2619-2623.
- [19] Y. Xue, Y. Chen, M.L. Zhang, Y.D. Yan, *Mater. Lett.* 62 (2008) 3884-3886.